*Anal. Chem.* **1995**, *67*, 3936–3944

# Aldehyde Biosensor Based on the Determination of NADH Enzymatically Generated by Aldehyde Dehydrogenase

**F. Pariente,† E. Lorenzo,† F. Tobalina,† and H. D. Abruña*,‡**

*Departamento de Química Analítica y Análisis Instrumental, Universidad Autónoma de Madrid, Canto Blanco 28049, Madrid, Spain, and Baker Laboratory, Department of Chemistry, Cornell University, Ithaca, New York 14853-1301*

**We describe the preparation, characterization, and performance of an aldehyde biosensor based on the determination of NADH generated by the enzymatic activity of immobilized (on a nylon mesh membrane) aldehyde dehydrogenase. The enzymatically generated NADH is, in turn, electrocatalytically oxidized at a glassy carbon electrode modified with an electropolymerized film of 3,4-dihydroxybenzaldehyde (3,4-DHB). We have characterized the response of the biosensor in terms of the effects of the immobilization procedure, enzyme loading, pH of the solution, and the presence of anionic species with particular emphasis on the role of phosphate anions. In addition, we have carried out studies of the kinetics of the catalytic reaction, as well as permeability studies. The sensor exhibits high sensitivity and a limit of detection in the micromolar regime (5.0 μM), as well as rapid response (60 s to reach 90% of its steady state value). We have also carried out analytical determinations of aliphatic and aromatic aldehydes and consistently find that aromatic aldehydes give superior results.**

There continues to be a great deal of interest in the development of materials capable of the electrocatalytic oxidation of NADH, in order to diminish the typically large overpotentials encountered in its direct oxidation at most electrode surfaces. Particular interest has centered on materials that can be immobilized onto electrode surfaces. This interest derives, in part, because of the very large number (over 300) of dehydrogenases that employ NADH as a cofactor.[1,2] In addition, because dehydrogenase activity can be employed in biosensor design, the coupling of such enzymatic activity with the ability to catalyze the product of such reactions (NADH) opens numerous possibilities in sensor design and development.

Numerous materials and procedures as well as several modified electrodes[3–5] have been identified for the electrocatalytic oxidation of NADH. Although most of these can react with NADH added to a solution, examples where the mediator or modifier reacts with enzymatically generated NADH are less common. In one of the more recent examples where enzymatically generated co-factors were detected, Willner and Riklin[6] reported on an amperometric biosensor utilizing the $NAD^+$ cofactor-dependent enzyme, malic enzyme, using a quinone–enzyme monolayer-modified electrode. In this work, they were able to detect enzymatically generated products. If enzyme activity, coupled to other cofactors, is to be exploited in biosensor design and development, new approaches for coupling these need to be developed.

We recently[7] reported that the electrooxidation of 3,4-dihydroxybenzaldehyde (3,4-DHB) on glassy carbon electrodes gives rise to stable redox-active electropolymerized films. These films exhibited very high and persistent electrocatalytic activity for the oxidation of NADH.

We have now combined the electrocatalytic activity of glassy carbon electrodes modified wity electropolymerized films of 3,4-DHB with the enzymatic activity of immobilized (on a nylon mesh) aldehyde dehydrogenase (ALDH) to develop an aldehyde biosensor. ALDH, with a molecular weight of about 200 000 and composed of four subunits, catalyzes the oxidation of a broad range of aromatic and aliphatic aldehydes to the corresponding carboxylic acids with the concomitant reduction of $NAD^+$ to NADH.[8] The sensor we describe herein is based on the determination of NADH enzymatically generated by the reaction of aldehyde dehydrogenase. We describe the preparation, characterization, and utility of such a sensor. The approach described here can, in principle, be extended to the use of other dehydrogenase enzymes, including alcohol and glutamate dehydrogenase, among others.

## EXPERIMENTAL SECTION

**A. Materials.** Aldehyde dehydrogenase (ALDH; EC 1.2.1.5, from baker's yeast) was obtained from Sigma Chemical Co. as a lyophilized powder containing 7.7 units of enzyme activity per milligram of protein or as an ammonium sulfate-stabilized solution containing 12.0 units/mg of protein. Both preparations were stored below 0 °C. Under these conditions, no loss of enzyme activity was observed for several months. 3,4-Dihydroxybenzaldehyde (3,4-DHB; 97% purity) from Aldrich Chemical Co. was

† Universidad Autónoma de Madrid.
‡ Cornell University.

(1) (a) Chenault, H. K.; Whitesides, G. M. *Appl. Biochem. Biotechnol.* **1987**, *14*, 147. (b) Dugas, H.; Penney, C. In *Bioorganic Chemistry*; Cantor, C. R., Ed.; Springer Verlag: New York, 1981; p 395.
(2) Willner, I.; Mandler, D. *Enzyme Microb. Technol.* **1989**, *11*, 467.
(3) Laval, J. M.; Bourdillon, C.; Moiroux, J. *J. Am. Chem. Soc.* **1984**, *106*, 4701.
(4) (a) Gorton, L. *J. Chem. Soc., Faraday Trans. 1* **1986**, *82*, 1245. (b) Persson, B. *J. Electroanal. Chem.* **1990**, *286*, 61.
(5) Gorton, L.; Persson, B.; Hale, P. D.; Bouguslavsky, L. I.; Karan, H. I.; Lee, H. S.; Skotheim, T.; Lan, H. L.; Okamoto, Y. In *Biosensors and Chemical Sensors*; Edelman, P. G., Wang, J., Eds.; ACS Symposium Series 487; American Chemical Society: Washington, DC, 1992; Chapter 6, p 56.
(6) Willner, I.; Riklin, A. *Anal. Chem.* **1994**, *66*, 1535.
(7) Pariente, F.; Lorenzo, E.; Abruña, H. D. *Anal. Chem.* **1994**, *66*, 4337.
(8) Clark, J. F.; Jacob, W. B. *J. Biol. Chem.* **1970**, *245*, 6072.



0003-2700/95/0367-3936$9.00/0 

recrystallized twice from water using activated charcoal. Oxidized and reduced forms of nicotine adenine dinucleotide ($NAD^+$ and NADH, grade III), glutaraldehyde (grade I, 50% aqueous solution), and bovine serum albumin (BSA, fraction V, 96% purity) were obtained from Sigma Chemical Co. and used as received. Benzaldehyde, 4-pyridinecarboxaldehyde, formaldehyde, acetaldehyde, and heptaldehyde used as substrates of ALDH were high-purity reagents (>99%) obtained from Aldrich Chemical Co. All other reagents were of at least analytical grade and were used as received. Tris and phosphate buffers (0.1 M) with 0.1 M $KNO_3$ were employed. Nylon mesh (Nytal) with 50 × 50 $\mu$m pores and 70 $\mu$m in thickness were employed for enzyme immobilization. Water was purified with a Millipore Milli-Q system. All solutions were prepared just prior to use.

**B. Apparatus.** Cyclic voltammetric and chronoamperometric studies were carried out with a BAS CV-27 potentiostat and a Linseys $X-Y$ recorder or a Nicolet digital oscilloscope. Teflon-shrouded glassy carbon electrodes (geometric area, 0.071 $cm^2$) were used as working electrodes. A coiled platinum wire served as the auxiliary electrode. All potentials are reported against a sodium saturated calomel electrode (SSCE) without regard for the liquid junction. A Pine Instruments rotating disk electrode system with a glassy carbon disk electrode (geometric area, 0.26 $cm^2$) was employed in rotating disk electrode experiments.

**C. Procedures. 1. Electrode Activation and Modification with 3,4-DHB.** Prior to each experiment, glassy carbon electrodes were polished and activated as described previously.[7] For modification, the activated electrodes were placed in a 0.5 mM solution of 3,4-DHB in Tris/0.1 M $KNO_3$ or phosphate buffer (pH 7.0 or 8.0), and the potential was held at about +0.20 V (depending on pH; vide infra) for 3 min. Subsequently, the modified electrode was rinsed with water and placed in fresh buffer solution. The potential was scanned for 3 min at 100 mV/s over the range of −0.20 to +0.25 V so as to obtain a stable redox response for the surface-immobilized film of 3,4-DHB. Surface coverages were determined from integration of the charge under the voltammetric wave.

**2. Enzymatic Immobilization on Nylon Meshes.** The solubilized ALDH preparation was used as received, whereas the ALDH available as a lyophilized powder was dissolved, prior to immobilization, in buffer containing at least 50% glycerol. In the absence of glycerol, we observed a complete loss of activity after the immobilization process. The presence of ammonium sulfate in the solubilized ALDH preparation did not appear to affect the immobilization procedure with glutaraldehyde. Nylon meshes were cut into 6.0 mm diameter disks, dipped in methanol, rinsed with water, and dried in an air stream prior to use. For enzyme immobilization, the following solutions were added to each disk: 2.0 $\mu$L of glutaraldehyde (2.5% v/v), 2.5 $\mu$L of BSA (1% w/v), and 5.0 $\mu$L of ALDH (0.1−0.5 unit in 50 mM phosphate buffer containing 50% (v/v) glycerol). The mixture was carefully homogenized on the surface of the disk. Gelification of glutaraldehyde and the protein was carried out at room temperature for 30 min and afterward at −4 °C overnight. The unreacted carboxaldehyde groups were inactivated by immersing the disks in 50 mL of 0.10 M phosphate buffer (pH 7.0) containing 0.10 M glycine for 15 min at room temperature. The disks were washed three times with 25 mL of fresh phosphate buffer (pH 7.0). After use, the disks were washed with phosphate buffer and stored at −4 °C in 50% (v/v) glycerol/0.10 M phosphate buffer solution.

**3. Electrocatalytic Oxidation of NADH.** Cyclic voltammetric studies of NADH oxidation at glassy carbon electrodes modified with electropolymerized films of 3,4-DHB were carried out at different sweep rates and in the presence of various anions. In these studies, the solutions employed were either 0.10 M Tris/0.10 M $NaNO_3$ or 0.10 M phosphate buffer (pH 8.0), and the sweep rate was varied from 5 to 625 mV/s over the range from −0.20 to +0.25 V. The pH value of 8 was chosen as it falls within the range over which the enzyme exhibits maximal activity. In addition, rotating disk electrode (RDE) and potential step chronoamperometric experiments were carried out in order to investigate permeability and other transport effects. RDE experiments were carried out by sweeping the potential at 5 mV/s from −0.20 to +0.25 V. The rotation rate ($\omega$) was varied from 0 to 4000 rpm. In the chronoamperometric experiments, the potential was stepped from −0.20 (where no electrochemical activity was observed for 3,4-DHB layers) to +0.25 V. In some instances (see below), the potential was stepped to a value beyond the direct oxidation of NADH. The resulting current/time transients were recorded on a digital oscilloscope and transferred to a personal computer for further analysis.

**4. Biosensor Preparation and Response.** The biosensor was assembled by securing, with a holed cap, an enzyme-modified nylon mesh disk (prepared as described above) over a glassy carbon electrode previously modified with a film of 3,4-DHB. The assembled biosensor was placed in buffer solution for 1−2 min prior to use to ensure solvent equilibration.

The biosensor response was assayed in buffer solution containing 2.0 mM EDTA. Control voltammograms were carried out in the absence of either $NAD^+$ or substrate (see results). For substrate (aldehydes) determinations, the sensor was placed in 3.0 mL of buffer solution, containing 2.0 mM EDTA, at an applied potential of +0.25 V. After the background current had decayed to a steady value, aliquots (typically microliter) of a stock solution of substrate (typically 50 mM) in buffer were added. After the mixture was stirred for 30 s and allowed 2 min for equilibration, the steady-state current (typically achieved in less than 60 s) in the unstirred solution was recorded.

## RESULTS AND DISCUSSION

**A. Biosensor Description.** The biosensor used in this work is schematically depicted in Figure 1. It consists of a 6 mm diameter nylon mesh disk modified with ALDH as described earlier. The disk is held over a glassy carbon electrode previously modified with an electropolymerized film of 3,4-DHB with a plastic cap with a 4 mm hole which defined the active area of the sensor. From optical microscopy studies (not shown), we have found that enzyme immobilization takes place preferentially on the fibers of the mesh, without occlusion of the pores. Under these conditions, transport to the electrode surface is not impeded, making this immobilization procedure superior to direct protein immobilization over the electrode surface as we have reported previously.[9] Moreover, in this assembly, the enzyme component is physically separated, thus allowing for its ready reuse with other electrodes.

The immobilized enzyme (ALDH) oxidizes aldehydes to the corresponding carboxylic acids in the presence of $NAD^+$. This cofactor acts as an acceptor of electrons generated in the enzymatic reaction and is transformed to its reduced form, NADH.

(9) Pariente, F.; Hernandez, L.; Lorenzo, E. *Bioelectrochem. Bioenerg.* **1992**, *27*, 73.

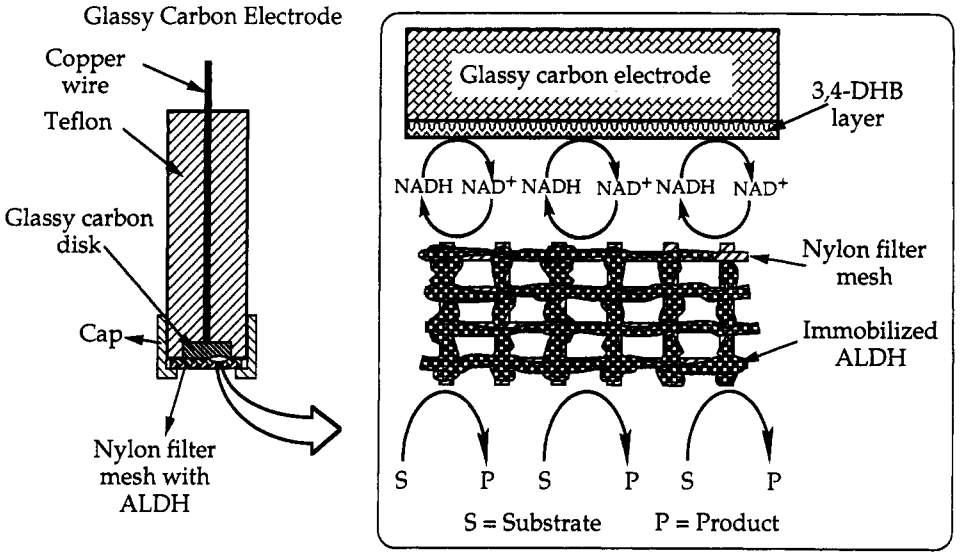


**Figure 1.** Schematic depiction of biosensor.

This, in turn, diffuses to the electrode, where it is catalytically reoxidized back to $NAD^+$ by the layer of electropolymerized 3,4-DHB (Figure 1). The 3,4-DHB-modified electrode serves as a secondary acceptor of electrons able to regenerate the cofactor ($NAD^+$) used in the enzymatic reaction so that the magnitude of this catalytic current can be employed as the analytical signal in the determination of the substrate (aldehyde) concentration.

To demonstrate that the $NAD^+$ generated by the catalytic oxidation of NADH by the electrodeposited film of 3,4-DHB is enzymatically active, we compared the currents for NADH oxidation at an electrode modified with 3,4-DHB only with the response for a biosensor in the presence of benzaldehyde. The current density for a biosensor with an $NAD^+$ concentration of 0.5 mM and 3.5 mM benzaldehyde is significantly larger than that for an electrode modified with 3,4-DHB alone in the presence of 0.5 mM NADH. The significantly larger current density for the biosensor indicates that the NADH generated (and which is subsequently oxidized to $NAD^+$) is enzymatically active and thus gives rise to the much larger catalytic currents. If the generated $NAD^+$ were not enzymatically active, such high catalytic currents would not be observed. In addition, we have carried out an experiment where a biosensor was removed from a solution containing $NAD^+$ and placed in one containing benzaldehyde but no $NAD^+$ in solution. A catalytic current is observed, and although it decreases with time (ostensibly due to diffusion of NADH/$NAD^+$ into the solution), the fact that a catalytic response is observed implies that the $NAD^+$ generated is enzymatically active.

**B. Electrochemical Characterization of NADH Oxidation at Electrodes Modified with an Electropolymerized Film of 3,4-DHB.** As we previously reported,[7] glassy carbon electrodes modified with an electropolymerized film of 3,4-DHB show the behavior anticipated for a surface-immobilized redox couple. As shown in Figure 2A, the voltammetric response had the expected wave shape for a surface-confined redox center with a small (although not zero) $\Delta E_p$ value. In addition, the current was directly proportional to the rate of potential sweep over the range of 25–500 mV/s, suggesting facile charge transfer kinetics. Virtually the same results were obtained in Tris/$KNO_3$ or phosphate buffers. As we have previously reported,[7] these films are quite stable as long as the applied potential does not exceed +0.40 V, where film degradation appears to take place. The

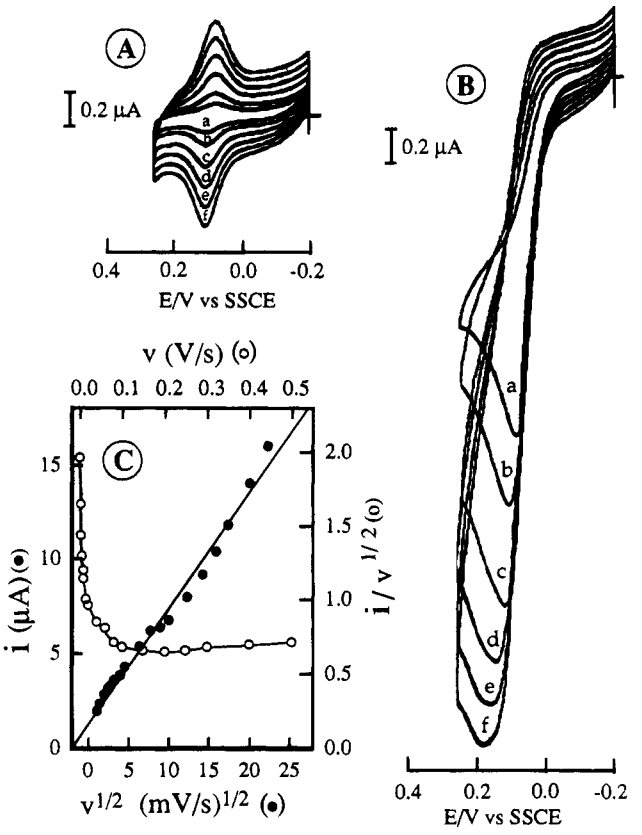


**Figure 2.** (A and B) Dependence of cyclic voltammetric response on sweep rate for a glassy carbon electrode modified with an electropolymerized film of 3,4-DHB in 0.1 M phosphate buffer (pH 7.0) in the absence (A) or in the presence (B) of 0.9 mM NADH. Sweep rates: a, 1.0; b, 2.0; c, 4.0; d, 6.0; e, 8.0; and f, 10.0 mV/s. (C) Variation of the catalytic current ($i$) with the square root of sweep rate (●) and variation of the sweep rate-normalized current $i/v^{1/2}$ with the sweep rate (○) for 3,4-DHB-modified electrodes in 0.1 M phosphate buffer (pH 7.0) in the presence of 0.9 mM NADH.

addition of NADH to the solution (Figure 2B) resulted in a dramatic change in the voltammogram, with a large enhancement of the anodic current and virtually no current in the reverse (cathodic) sweep. It can also be noted in Figure 2B that the peak potential for the catalytic oxidation of NADH shifts to more positive potentials as the sweep rate is increased, suggesting a kinetic

**Scheme 1**

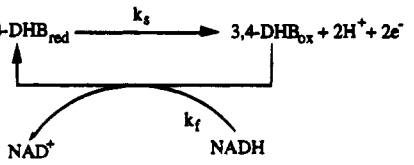


limitation in the reaction between the electropolymerized film of 3,4-DHB and NADH. However, a plot of the catalytic peak current vs the square root of the sweep rate is linear (Figure 2C(●)), suggesting that at sufficient overpotentials the reaction is transport limited.

A plot of the sweep rate-normalized current ($i/v^{1/2}$) vs sweep rate (Figure 2C (○)) exhibits the characteristic shape typical of an $EC_{cat}$ process, as depicted in Scheme 1, where $k_s$ is the heterogeneous charge transfer rate constant and $k_f$ is the pseudo-first-order rate constant. Andrieux and Saveant[10] developed a theoretical model for such a mechanism and derived a relation (eq 1) between the peak current and the concentration of the

$$i_{cat} = 0.496nFAD_s^{1/2}v^{1/2}C_s^*(nF/RT)^{1/2} \quad (1)$$

substrate for the case of slow sweep rate ($v$) and large $k_f$, where $D_s$ and $C_s^*$ are the diffusion coefficient (cm$^2$/s) and the bulk concentration (mol/cm$^3$) of the substrate (NADH in this case), respectively, and the other symbols have their usual meanings. Low values of $k_f$ result in values lower than 0.496 for the constant. For low sweep rates (1.0–10.0 mV/s), we find the average value of this constant to be 0.35 for a 3,4-DHB-modified electrode with a coverage of $\Gamma = 3.3 \times 10^{-10}$ mol/cm$^2$ in the presence of 0.93 mM NADH. According to the approach of Andrieux and Saveant and using Figure 1 in their theoretical paper,[10] we calculate a value of $k_f = 2.6 \times 10^3$ M$^{-1}$ s$^{-1}$. This value is of the same order of magnitude as those previously reported by several authors for electrooxidation of NADH at graphite electrodes modified with catechol functionalities.[11,12] Since in all of these cases the active component is an *o*-quinone moiety, the similarity of these values suggests that the measured rate constant is inherent to the reaction.

**C. Rotating Disk Electrode Experiments.** Kinetic parameters were also obtained from RDE measurements. The catalytic current, $i$, for NADH oxidation at 3,4-DHB-modified electrodes was measured in 0.1 M phosphate buffer solutions (pH 8.0) containing 0.10 mM NADH. The results for an electrode with a coverage of $2.0 \times 10^{-10}$ mol/cm$^2$ are shown in Figure 3. The current increased with increasing rate of rotation, $\omega$, up to about 500 rpm and then leveled off. Also, a plot of $i$ vs $\omega^{1/2}$ (i.e., a Levich plot) was found to be nonlinear, suggesting kinetic limitations. In addition, at lower NADH concentrations, the current was proportional to $\omega^{1/2}$ over a larger range of rotation rates, although at sufficiently large values, they all leveled off. These are the anticipated results for a system that is under kinetic control.[13,14]

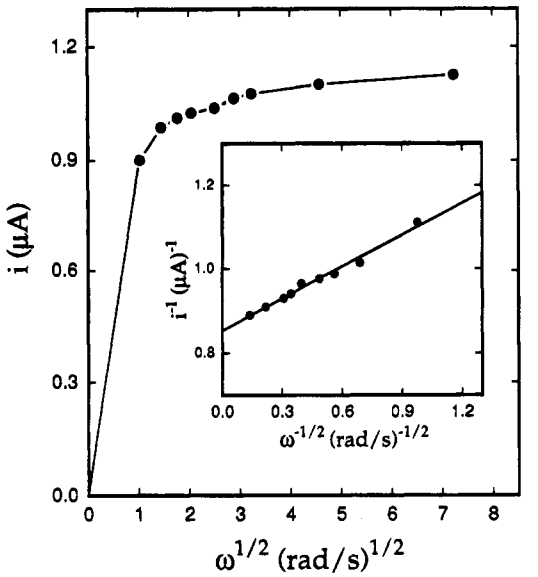


**Figure 3.** Electrocatalytic current, at an applied potential of +0.25 V, vs $\omega^{1/2}$ for 0.1 mM NADH oxidation at a 3,4-DHB-modified glassy carbon rotating disk electrode in 0.1 M phosphate buffer (pH 8.0). The coverage was $2.0 \times 10^{-10}$ mol/cm$^2$. (Inset) Plot of $1/i$ vs $1/\omega^{1/2}$ (Koutecky–Levich plot).

Since at +0.20 V the rate of oxidation of the electropolymerized film of 3,4-DHB on the electrode can be considered fast, this would suggest that the oxidation of the NADH (Scheme 1) is the rate-determining step. Under these conditions, the Koutecky–Levich equation can be used to determine the rate constant for the process. The Koutecky–Levich equation can be formulated as follows:

$$1/i_{lim} = 1/(nFAk\Gamma C_b) + 1/(0.62nFAv^{-1/6}D^{2/3}\omega^{1/2}C_b) \quad (2)$$

where $C_b$ is the bulk concentration of the reactant (NADH) in solution, $\Gamma$ is the total surface coverage, $\nu$ is the kinematic viscosity, $\omega$ is the rate of rotation and $k$ is the rate constant, with all other symbols having their conventional meanings. From eq 2, it is apparent that the value of $k$ can be determined from the intercept of a plot of $1/i_{lim}$ vs $1/\omega^{1/2}$ (or a so-called Koutecky–Levich plot). Such a plot (Figure 3, inset), obtained from the experimental data in the main panel in Figure 3, shows the anticipated linear dependence. From the value of the intercept, $k_f$ was found to be $2.7 \times 10^3$ M$^{-1}$ s$^{-1}$, which is virtually identical to that determined from cyclic voltammetric measurements.

**D. Permeability of NADH.** Using potential step chronoamperometry, we have determined the diffusion coefficient of NADH at glassy carbon electrodes modified with an electropolymerized film of 3,4-DHB and in the presence or absence of the nylon filter mesh which was modified as previously described. In chronoamperometric studies, the current, $i$, for the electrochemical reaction (at a mass transport-limited rate) of an electroactive material (NADH in this case) that diffuses to an electrode through a film barrier with a diffusion coefficient, $D$ (which maybe different from the value in solution), is described by the Cottrell equation,

$$i = \frac{nFAD^{1/2}C_{NADH}^*}{\pi^{1/2}t^{1/2}} \quad (3)$$

where $D$ is the diffusion coefficient and $C^*$ is the bulk concentration

(10) Andrieux, C. P.; Savéant, J.-M. *J. Electroanal. Chem.* **1978**, *93*, 163.
(11) Jaegfeldt, H.; Tortensson, A. B. C.; Gorton, L. G.; Johansson, G. *Anal. Chem.* **1981**, *53*, 1979.
(12) Jaegfeldt, H.; Kuwana, T.; Johansson, G. *J. Am. Chem. Soc.* **1983**, *105*, 1805.
(13) Andrieux, C. P.; Dumas-Bouchiat, J. M.; Savéant, J.-M. *J. Electroanal. Chem.* **1980**, *114*, 159.
(14) Andrieux, C. P.; Dumas-Bouchiat, J. M.; Savéant, J.-M. *J. Electroanal. Chem.* **1984**, *169*, 9.

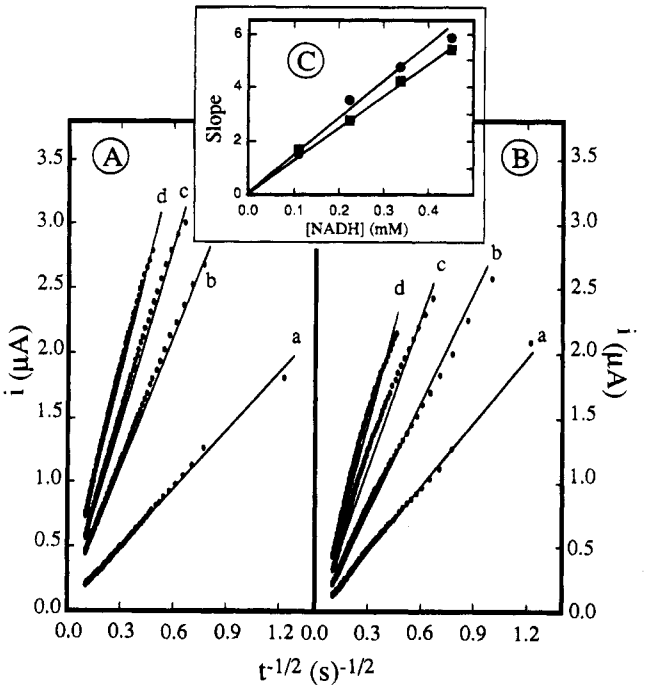


**Figure 4.** (A and B) Plots of $i$ vs $t^{-1/2}$ obtained from chronoamperometric experiments for a 3,4-DHB-modified electrode (A) or for a 3,4-DHB/ALDH biosensor (B) in 0.1 M phosphate buffer solutions (pH 8.0) containing NADH at concentrations of a, 0.113; b, 0.226; c, 0.34; and d, 0.45 mM. Lines are the best fits to the data. (C) Plot of the slopes of the straight lines from A and B against the NADH concentration for the 3,4-DHB-modified electrode (●) and for the 3,4-DHB/ALDH biosensor (■).

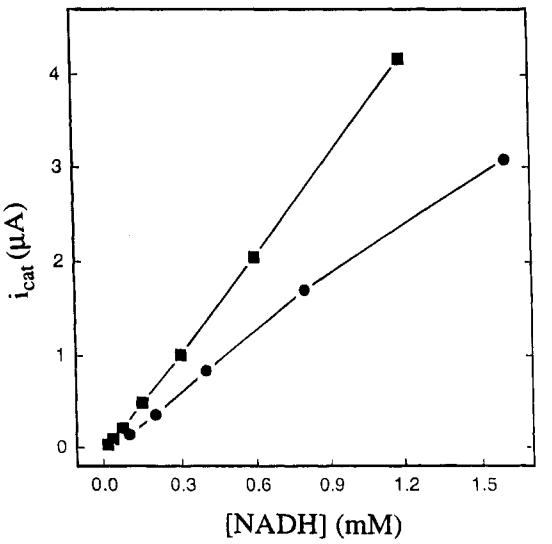


**Figure 5.** Calibration curves ($i$ vs [NADH]) for a 3,4-DHB-modified glassy carbon electrode in 0.1 M phosphate (■) or 0.1 M Tris/0.1 M $NaNO_3$ (●) buffer solutions (pH 8.0).

in mol/cm$^3$.[15] Under diffusion (mass transport) control, a plot of $i$ vs $1/t^{1/2}$ will be linear, and from the slope, the value of $D$ can be obtained. We have carried out such studies at various NADH concentrations, for glassy carbon electrodes modified with electropolymerized films of 3,4-DHB in the absence (Figure 4A) and in the presence (Figure 4B) of the modified nylon filter mesh in phosphate buffer (pH 8.0). Parts A and B of Figure 4 show the experimental plots along with the best fits for the different concentrations of NADH employed. The slopes of the resulting straight lines were then plotted vs the NADH concentration (Figure 4C), from whose slopes we calculated diffusion coefficients of $2.67 \times 10^{-6}$ and $2.14 \times 10^{-6}$ cm$^2$/s for NADH in the absence and presence of the nylon filter mesh, respectively. In order to unambiguously establish that the oxidation of NADH is transport limited, we also carried out experiments where the potential was stepped to values where the direct oxidation of NADH was transport limited. The results obtained were virtually identical to those where the potential was stepped beyond the value for the surface-immobilized film of 3,4-DHB, suggesting that under those conditions, the process was indeed transport limited. These results indicate that the presence of the filter mesh results in a diminution in the transport of NADH of about 20%, so the present procedure for enzyme immobilization is very well suited for biosensor applications because of the relatively small decrease in transport rates.

**E. Optimal Conditions for Catalytic Oxidation of NADH at 3,4-DHB-Modified Glassy Carbon Electrodes.** Since this biosensor combines two kinetic reactions (enzymatic and electrochemical), experimental conditions compatible with both processes are required. Of particular importance are the optimal conditions for the enzymatic reaction, which is a key component of the sensor. ALDH requires the presence of relatively high concentrations of potassium ions for its activity.[16] Heavy metals, especially $Cu^{2+}$, strongly inhibit its activity.[17] In addition, the enzyme is active from pH 7.0 to 9.0, although pH 8.75 has been reported to be optimal.[16] For these reasons, in all studies of the biosensor, we employed buffers containing 0.1 M potassium ions and 2.0 mM EDTA (so as to complex any trace $Cu^{2+}$ ions). In addition, the pH studies were restricted to a range around the optimal pH described for this enzyme.

Tris or phosphate buffers gave the best results in terms of levels of activity for NADH in solution. To determine the optimal buffer for the experiments, we carried out a comparative study of the oxidation of NADH, at different concentrations, at glassy carbon electrodes modified with electropolymerized films of 3,4-DHB over the pH range of 7.0 to 9.0. When phosphate buffers were employed, the catalytic activity of the films was 20% higher than in the presence of Tris buffers, and the linear range of the response was wider (Figure 5). These effects were observed over the entire pH range studied. We have previously observed similar effects of the nature of the supporting electrolyte anions on the electrochemical response of a self-assembling quinone derivative used as a surface-immobilized material for the catalytic electrooxidation of NADH.[18] In that study, we observed that the addition of phosphate or acetate buffers resulted in better defined waves as well as an apparent enhancement of the surface coverage in addition to an enhancement in the electrocatalytic current. Although we are, at this time, uncertain as to the origin of these effects, they might be due to an enhancement in the charge transport properties of the film. Based on these results, phosphate buffers were employed in all further experiments.

As we reported previously,[7] the electropolymerization of 3,4-DHB and the redox response of the resulting electropolymerized

(15) Bard, A. J.; Faulkner, L. R. *Electrochemical Methods*; Wiley: New York, 1980.

(16) Black, S. In *Methods in Enzymology, Vol. I*; Colawic, S. P., Kaplan, N. O., Eds.; Academic Press: New York, 1955; p 508.

(17) Jacobsen, M. K.; Bernofsky, C. *Biochim. Biophys. Acta* **1974**, *350*, 277.

(18) Lorenzo, E.; Sánchez, L.; Pariente, F.; Tirado, J.; Abruña, H. D. *Anal. Chim. Acta* **1995**, *309*, 79.

**Table 1. Variations in the Properties of Electropolymerized Films of 3,4-DHB in Phosphate Buffers as a Function of Deposition Potential and pH**

| pH | $E_{dep}$[a] | $I_{p,a}$[b] | $I_{p,c}$[b] | $E_{p,a}$[c] | $E_{p,c}$[c] | $\Delta E_p$[d] | $E^{o'}$[e] | $\Gamma$[f] |
|---|---|---|---|---|---|---|---|---|
| 7.0 | +0.25 | 4.7 | 4.7 | +0.150 | +0.100 | 50 | +0.125 | 3.60 |
| 7.5 | +0.23 | 4.4 | 4.4 | +0.115 | +0.080 | 35 | +0.100 | 3.46 |
| 8.0 | +0.20 | 4.2 | 4.0 | +0.100 | +0.075 | 25 | +0.088 | 3.30 |
| 8.5 | +0.15 | 3.9 | 3.8 | +0.060 | +0.030 | 30 | +0.045 | 2.71 |
| 9.0 | +0.13 | 3.6 | 3.2 | +0.040 | +0.015 | 25 | +0.028 | 2.52 |

[a] Deposition potential in volts vs SSCE. [b] Anodic (a) and cathodic (c) peak currents in microamperes. [c] Anodic (a) and cathodic (c) peak potentials in volts vs SSCE. [d] Defined as $E_{p,a} - E_{p,c}$, in millivolts. [e] Formal potential defined as $(E_{p,a} + E_{p,c})/2$ in volts vs SSCE. [f] Surface coverages in mol/cm$^2$ $\times$ $10^{10}$.

material are strongly pH dependent in Tris/nitrate buffers. To determine if such effects were also present here, we studied, in phosphate buffers, the effects of the deposition potential and pH over the range of 7.0–9.0 on the voltammetric response and the properties of the 3,4-DHB-modified electrodes. Table 1 shows representative data. In general, for pH values above 7.0, a decrease in the apparent surface coverage is observed. Since the p$K_a$ for 3,4-dihydroxybenzaldehyde is 7.21,[19] above this pH value the material will be present in its deprotonated form, and this might be responsible for the observed effect. However, this apparent decrease in the surface coverage observed at pH values above 7.0 (Figure 6B) does not involve a dramatic decrease in the sensitivity of the modified electrode for the catalysis of NADH oxidation, as can be ascertained from the calibration curves presented in Figure 6A. Although the slopes of the calibration curves decrease with increasing pH, the changes are not dramatic. In addition, the linear range of the response remained virtually unchanged and reached values of up to 1.2–1.5 mM (Figure 6A).

Moreover, the coverage-normalized response ($i/\Gamma$) actually increases at pH values above 8 (Figure 6C), suggesting that whereas the apparent coverage decreases, the material has a higher activity. These results suggest a more effective interaction of the NADH with the *o*-quinone groups of the 3,4-DHB film at slightly basic pH as opposed to neutral or acidic pH.

We have also carried out a series experiments intended to address potential interferences by ascorbate, uric acid, and acetaminophen by determining the current response of glassy carbon electrodes modified with 3,4-DHB in the presence of 1 mM NADH and in the presence or absence of potential interferents at varying concentrations. Whereas uric acid and acetaminophen presented no interference effects at concentrations up to 10-fold higher than the NADH concentration, ascorbate did present interference effects which were concentration dependent. At NADH/ascorbate concentration ratios of 10:1, the interference due to ascorbate was of the order of 1.5%. However, at comparable concentrations, the interference effects were more marked (80% at 1.0 mM ascorbate concentration). We have carried out some preliminary experiments where the electrode assembly is coated with a thin film of Nafion, and it appears that this might suppress these interference effects.

**F. 3,4-DHB/ALDH Biosensor Response.** One of the objectives of these investigations was the development of biosensors based on dehydrogenase activity. To test for the potential utility in biosensors of glassy carbon electrodes modified with

(19) Slabbert, N. P. *Tetrahedron* **1977**, *33*, 821.

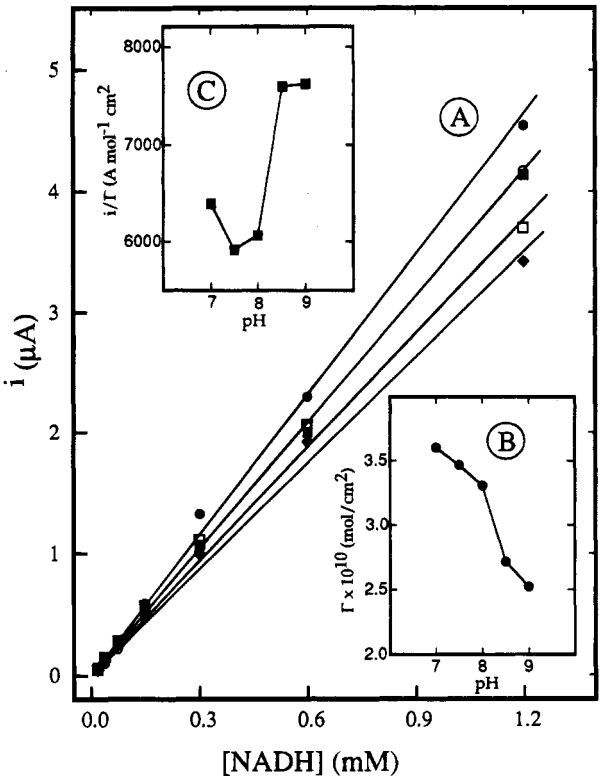


**Figure 6.** (A) Effect of pH (0.10 M phosphate buffer) on the electrocatalytic oxidation of NADH at 3,4-DHB-modified glassy carbon electrodes. pH values were (●) 7.0, (○) 7.5, (■) 8.0, (□) 8.5, and (◆) 9.0. (B) Effect of pH on the apparent coverage of 3,4-DHB. (C) Variation of the coverage-normalized current ($i/\Gamma$) with pH in 0.10 M phosphate buffer solutions containing 0.6 mM NADH.

electropolymerized films of 3,4-DBH, we employed them in conjunction with immobilized (on a nylon filter mesh) aldehyde dehydrogenase (ALDH). The intent was to couple the enzymatic activity (toward aldehydes) of ALDH with the electrocatalytic activity of the 3,4-DHB films toward NADH oxidation. Initial studies were performed with benzaldehyde as substrate. The cyclic voltammetric response (at slow sweep rate) of the biosensor in the presence and absence of benzaldehyde was used to assess the activity of the biosensor.

Figure 7A, trace a, shows the cyclic voltammetric response at 5 mV/s for a biosensor incorporating 0.5 unit of immobilized AlDH and in contact with a pH 8 phosphate buffer solution containing 2 mM EDTA and 1 mM $NAD^+$ but in the absence of benzaldehyde. The characteristic and well-behaved redox response for the 3,4-DHB polymer film on the electrode is readily apparent. Upon the addition of benzaldehyde to a concentration of 50 $\mu$M, an enhancement of the anodic current (Figure 7A, trace b) is clearly noted. Additional increases in the concentration of benzaldehyde to 100 (c), 200 (d), 300 (e), 400 (f), 500 (g), and 600 $\mu$M (h) resulted in concomitant increases in the anodic peak current. At NADH concentrations of 300 $\mu$M and above, there is no current in the return (cathodic) sweep, consistent with a high degree of electrocatalytic activity for the enzymatically generated NADH. In addition, the biosensor response was linear from 50 to 400 $\mu$M benzaldehyde. Over this concentration range, the response was very similar to that obtained for NADH added to the solution (see Figure 5), suggesting that the biosensor response is under mass transport control and that virtually all of the NADH generated by the enzymatic reaction is immediately reoxidized

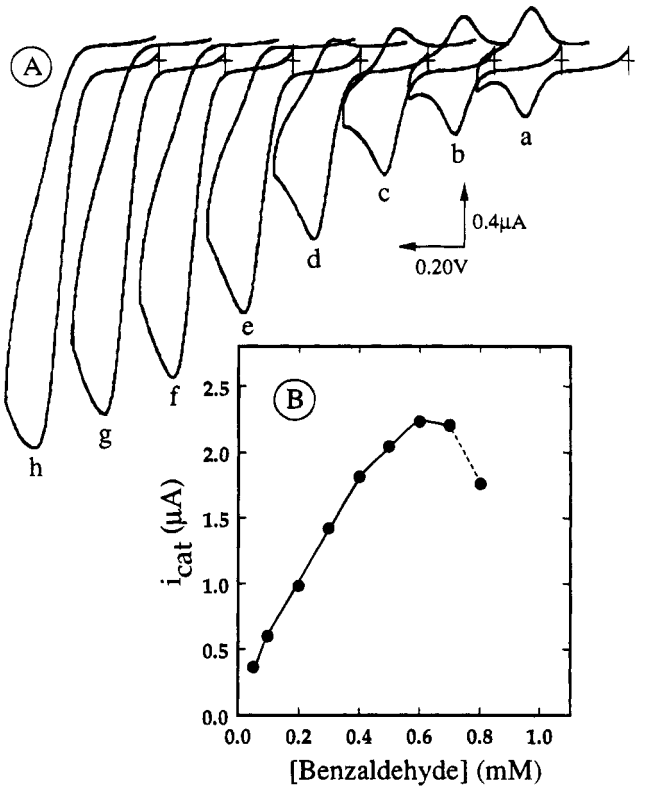


**Figure 7.** (A) Cyclic voltammetric response at 5 mV/s for a 3,4-DHB/ALDH biosensor with 0.5 unit of immobilized ALDH in 0.1 M phosphate buffer (pH 8.0), 2.0 mM EDTA, and 1.0 mM $NAD^+$ as a function of benzaldehyde concentration: (a) none, (b) 50.0, (c) 100, (d) 200, (e) 300, (f) 400, (g) 500, and (h) 600 $\mu$M. (B) Catalytic current ($i_{cat}$) vs benzaldehyde concentration.

by the 3,4-DHB layer on the glassy carbon electrode. Concentrations of benzaldehyde higher than 0.6 mM (Figure 7B) caused a dramatic decrease in the response, probably due to an inhibitory effect of the ALDH activity by excess substrate. A similar inhibitory effect has been reported for this enzyme in solution when acetaldehyde was used as substrate.[17]

For immobilized enzymes used in amperometric biosensors, the observed electrochemical response may be either mass transport limited or kinetically controlled.[20] Mell and Malloy suggested that for an immobilized enzyme reaction that is kinetically controlled, the steady state current, $i_{ss}$, is proportional to the initial rate of the enzymatic process. In this case, a plot of $i_{ss}$ vs the substrate concentration, $C_s$, gives a typical Michaelis–Menten-type response. In addition, a linear double reciprocal plot (or a so-called Lineweaver–Burk plot) of $1/i_{ss}$ vs $1/C_s$ will be diagnostic of kinetic control of the electrochemical response. Figure 8 shows the steady state currents obtained at +0.25 V for increasing concentrations of benzaldehyde employing a biosensor with 0.5 units of ALDH immobilized on the nylon mesh. The $i_{ss}$ vs $C$ plot exhibits the typical Michaelis–Menten shape with a saturation response being reached for benzaldehyde concentrations above 0.5 mM. The double reciprocal plot (inset) is linear over the benzaldehyde concentration range studied. These results suggest control by the enzymatic reaction, and the apparent Michaelis–Menten constant, $K'_m$, was calculated to be 0.55 mM.

**G. Effect of pH on the Biosensor Response.** As was mentioned before and as depicted in Figure 6C for the catalytic

(20) Mell, L. D.; Malloy, J. T. *Anal. Chem.* **1975**, *47*, 299.

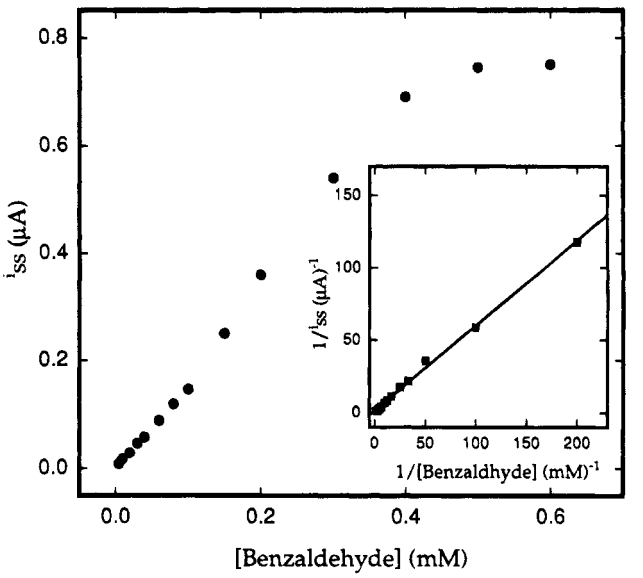


**Figure 8.** Steady state current at +0.25 V and double reciprocal (Lineweaver–Burk) plot (inset) for a 3,4-DHB/ALDH biosensor containing 0.5 unit of immobilized ALDH in the presence of increasing concentrations of benzaldehyde. Other experimental conditions as in Figure 7.

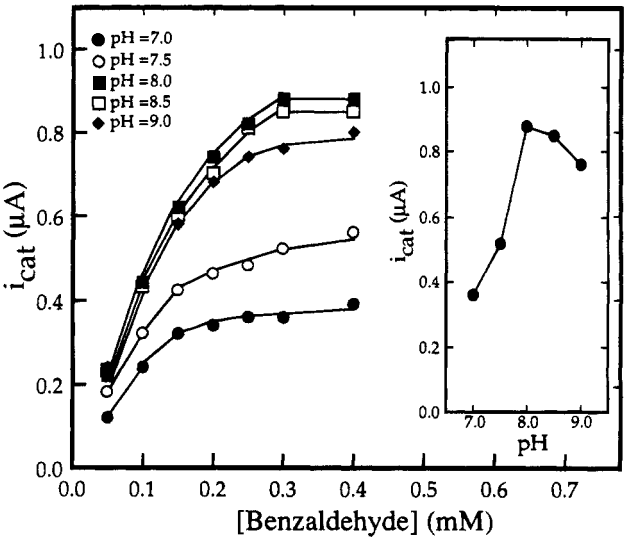


**Figure 9.** Voltammetric response, at various pH values, of the 3,4-DHB/ALDH biosensor containing 0.5 unit of immobilized ALDH as a function of benzaldehyde concentration. Other experimental conditions as in Figure 7. (Inset) Current vs pH response for a 3,4-DHB/ALDH biosensor containing 0.5 unit of immobilized ALDH at a benzaldehyde concentration of 300 $\mu$M. Other experimental conditions as in Figure 7.

oxidation of NADH at 3,4-DHB-modified electrodes, the best normalized current response ($i/\Gamma$) was obtained in the interval of pH between 8.0 and 9.0. To determine the pH dependence of the biosensor response, we monitored the current (at +0.25 V) at different pH values and for noninhibitory concentrations of benzaldehyde, and the results are presented in Figure 9.

The biosensor exhibits a marked increase in response above pH 7.5, with the highest response being achieved from pH 8 to 8.5 (Figure 9). Above pH 9.0, there is a significant decrease in response. The inset to Figure 9 depicts the biosensor response as a function of pH at a benzaldehyde concentration of 300 $\mu$M. From this plot, it is evident that the optimal response is attained at a pH of 8, so further studies were carried out at this pH value.

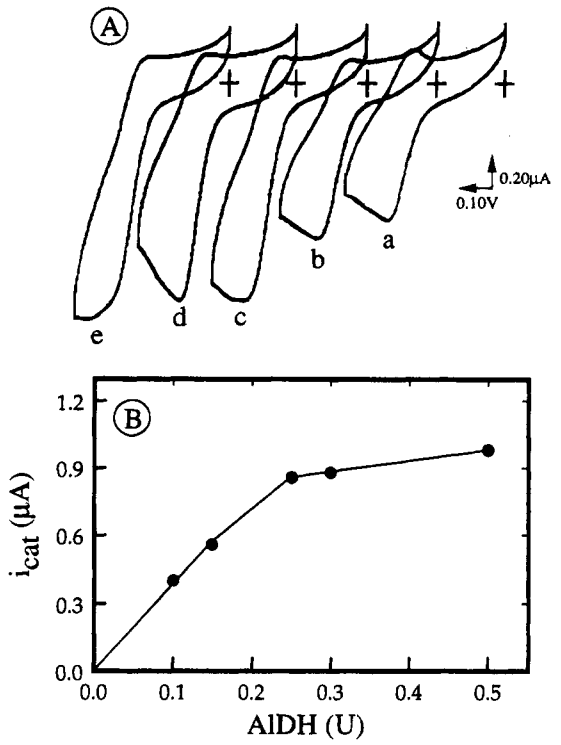


**Figure 10.** (A) Effect of ALDH loading on the voltammetric response to substrate (0.3 mM benzaldehyde) of 3,4-DHB/ALDH biosensors performed with filter meshes containing (a) 0.1, (b) 0.15, (c) 0.25, (d) 0.3, and (e) 0.5 unit of immobilized ALDH. (B) Plot of peak current against the ALDH units loaded in each biosensor. Other experimental conditions as in Figure 7.

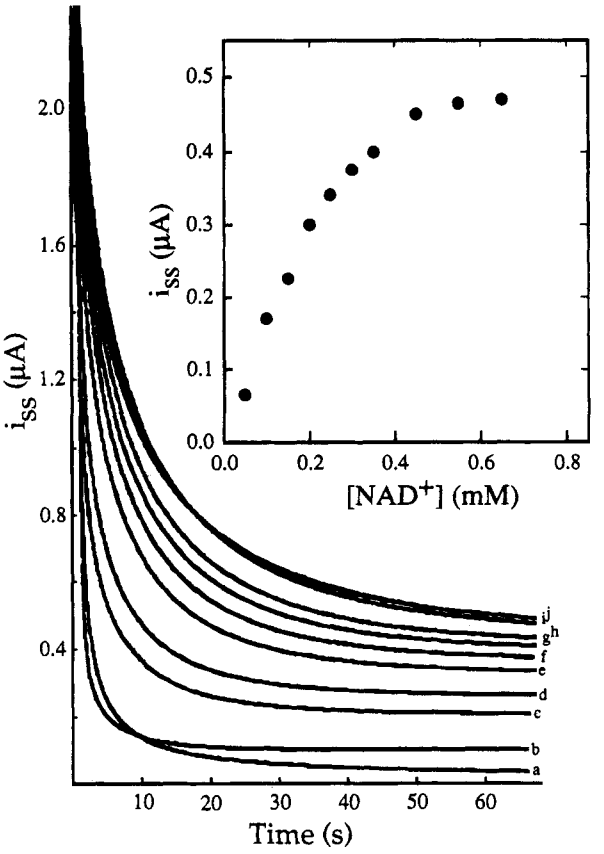


**Figure 11.** Current–time transients for the oxidation of 0.35 mM benzaldehyde at a 3,4-DHB/ALDH biosensor containing 0.5 unit of immobilized ALDH in the presence of $NAD^+$ at concentrations of (a) 50, (b) 100, (c) 150, (d) 200, (e) 250, (f) 300, (g) 350, (h) 450, (i) 550, and (j) 650 μM. (Inset) Plot of steady state current as a function of $NAD^+$ concentration.

**H. Effect of Enzyme Loading and $NAD^+$ Concentration on Biosensor Response.** The response of the 3,4-DHB/ALDH biosensor will be dependent on the amount of active ALDH immobilized. Figure 10A shows the voltammetric response for biosensors prepared with increasing amounts of immobilized ALDH, to a constant concentration (0.3 mM) of benzaldehyde in solution. At loadings below 0.25 unit (traces a and b), an increase in response with enzyme loading is evident, but at higher loadings (d and e), the response levels off, suggesting a saturation response. Figure 10B shows a plot of catalytic current as a function of enzyme loading where the above-mentioned trends are clear, with the response increasing linearly at low loadings and reaching a saturation response for enzyme loadings above 0.25 units. In order to obtain a sensor with a long lifetime and to account for possible losses of enzymatic activity, which would affect reproducibility, an enzyme loading level of 0.5 unit was deemed optimal and was thus employed in all further studies.

The effect of $NAD^+$ concentration on the response was studied using a biosensor with 0.5 unit of immobilized ALDH and at a benzaldehyde concentration of 300 μM; the results are presented in Figure 11. In the main panel are presented the current–time profiles after the application of a potential of +0.25 V under the above-mentioned conditions and for increasing concentrations of $NAD^+$. It is evident that there is an increase in the steady state current plots for increasing concentrations of $NAD^+$. The inset to Figure 11 shows a plot of the steady state current as a function of $NAD^+$ concentration, where it is apparent that for concentrations below 0.3 mM there is an increase in the response with concentration, whereas the response levels off for concentrations above 0.35 mM. Based on these results and in order to ensure that the response of the biosensor was independent of $NAD^+$ concentration, a value of 1 mM was employed in analytical determinations.

Another point to be considered from the data in Figure 11 is the response time for the sensor. In the family of current–time response curves, it is clear that in all cases a steady state response is reached within 60 s. Since the benzaldehyde concentration used in these studies (300 μM) was at the onset of a saturation response for the enzyme, it implies that the biosensor will have, in general, rapid response times which is a very valuable aspect in analytical determinations.

**I. Analytical Determinations of Various Aldehydes with the 3,4-DHB/ALDH Biosensor.** Amperometric enzyme biosensors are systems that combine the specificity of enzyme catalysis with the high sensitivity of electrochemical methods. To test for substrate sensitivity effects, various aldehydes were used as substrate for the 3,4-DHB/ALDH biosensor. The specific substrates employed were benzaldehyde, 4-pyridinecarboxaldehyde, heptaldehyde, formaldehyde, and acetaldehyde. These substrates were chosen so that comparisons could be made between the responses for aromatic vs aliphatic aldehydes and, in the latter, in terms of short (formaldehyde, acetaldehyde) vs long (heptaldehyde) aliphatic chains. In these studies, the optimized parameters previously established were employed. The catalytic peak currents obtained at different substrate concentrations were used in constructing response curves, and the results are presented in Figure 12. As is evident from the figure, the

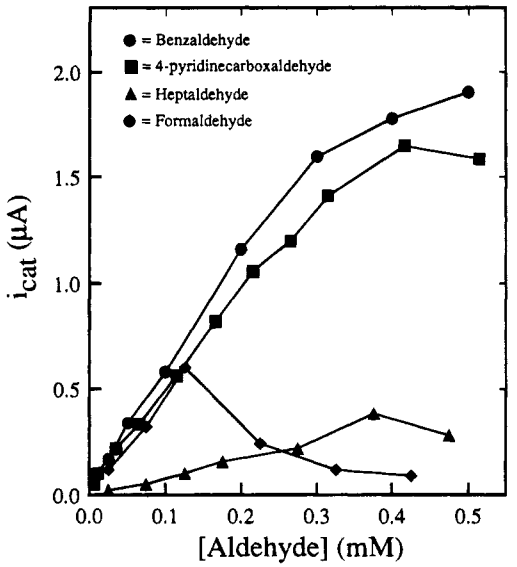


**Figure 12.** Catalytic current in 0.1 M phosphate buffer (pH 8.0) of 3,4-DHB/ALDH biosensors containing 0.5 unit of immobilized ALDH when different aldehydes were used as substrate. Other experimental conditions as in Figure 7.

best responses were obtained for aromatic aldehydes such as 4-pyridinecarboxaldehyde and benzaldehyde. In addition, inhibiting effects were apparent for all aldehydes, but the effects were more pronounced for the aliphatic ones. Moreover, heptaldehyde, with the longest aliphatic chain, had the lowest response of all substrates tested. Formaldehyde and acetaldehyde (the latter not shown in Figure 12) showed virtually identical responses, suggesting that for short-chain aliphatic aldehydes, the chain length does not appear to strongly affect the response.

Although ALDH from baker's yeast, as used in this work, has been reported to have a low affinity in solution for formaldehyde and acetaldehyde relative to ALDH from liver,[17] changes in the enzyme environment generated during the immobilization process and possible slight modifications of the active center could also be responsible, at least in part, for the decrease in the affinity for these aldehydes. As mentioned above, heptaldehyde exhibited the lowest response. This material has a very low solubility in aqueous media and can, furthermore, generate micelles which would be anticipated to have a very low affinity for the enzyme's active center, and this could, in part, be responsible for the very low response observed for this aldehyde. Perhaps the use of nonaqueous systems or surfactant solutions could enhance the response by minimizing micelle formation, and we are currently exploring such approaches.

It is clear that this approach to biosensor design can, in principle, be extended to other dehydrogenases, and we are currently involved in the development of biosensors based on the enzymatic activity of alcohol and lactate dehydrogenases. The results of these investigations will be reported elsewhere.

## CONCLUSIONS

We have prepared and characterized the performance of an aldehyde biosensor based on the determination of NADH generated by the enzymatic activity (toward aldehydes) of aldehyde dehydrogenase immobilized on a nylon mesh membrane. The analytical signal is based on the electrocatalytic oxidation, at a glassy carbon electrode modified with an electropolymerized film of 3,4-dihydroxybenzaldehyde, of the enzymatically generated NADH. We have characterized the response of the biosensor in terms of the effects of the immobilization procedure, enzyme loading, pH of the solution, and the presence of anionic species. We find that the immobilization procedure gives rise to only a small decrease (~20%) in transport rates, making it very appealing for biosensor applications. An enzyme loading of 0.5 unit and a pH of 8 gave the best performance. Phosphate anions enhance the response, and we believe this to be due to improved charge propagation. The sensor exhibits high sensitivity and a limit of detection in the micromolar regime (5.0 $\mu$M), as well as rapid response (60 s to reach 90% of its steady state value). We have also carried out analytical determinations of aliphatic and aromatic aldehydes and consistently find that aromatic aldehydes give superior results relative to aliphatic aldehydes, with long-chain aldehydes (heptaldehyde) giving the lowest response.

## ACKNOWLEDGMENT

This work was supported by the DGICYT of Spain through Grants BIO 93-0660C04-02 (E.L., F.P.F.T.) and PB92-0167 (H.D.A.), the National Science Foundation (DMR-9107116; H.D.A.), and a NATO Collaborative Research Grant (91-0047; H.D.A., E.L.).

Received for review February 27, 1995. Accepted August 18, 1995.[⊗]

AC950207O

[⊗] Abstract published in *Advance ACS Abstracts,* October 1, 1995.